Distinct Behavior of Connexin56 and Connexin46 Gap Junctional Channels Can Be Predicted from the Behavior of their Hemi-Gap-Junctional Channels

Lisa Ebihara,* Viviana M. Berthoud,[‡] and Eric C. Beyer[‡]

*Department of Pharmacology, Columbia University, New York, New York 10032, and [‡]Department of Pediatrics, Washington University School of Medicine, St. Louis, Missouri 63110 USA

ABSTRACT   The gap-junctional protein rat connexin46 (Cx46) has the unusual ability to form voltage-gated channels in the nonjunctional plasma membrane of Xenopus oocytes (Paul et al., 1991; Ebihara and Steiner, 1993). These have been suggested to be gap-junctional hemichannels or connexons. The Xenopus oocyte system was used to characterize the functional properties of a closely related lens gap-junctional protein, chicken connexin56 (Cx56) (Rup et al., 1993) and to contrast them to those of rat Cx46. Single oocytes injected with either Cx56 or Cx46 cRNA developed time-dependent, outward currents that activated on depolarization. The currents induced by Cx56 and Cx46 showed differences in steady-state voltage dependence and in their degree of rectification. Furthermore, the voltage-dependent properties of the nonjunctional channels induced by the connexin cRNAs in external solutions containing low concentrations of calcium ions could account remarkably well for the behavior of the intercellular channels formed by Cx56 and Cx46 in paired oocytes. These results suggest that many of the voltage-dependent properties of the hemi-gap-junctional channels are retained by the intercellular channels.

INTRODUCTION

Gap junctions are composed of intercellular channels that allow the passage of ions and other small molecules between neighboring cells. The intercellular channels are comprised of a family of closely related proteins called connexins. At least 12 mammalian connexins have been cloned (Paul, 1986; Beyer et al., 1987; Zhang and Nicholson, 1989; Willecke et al., 1991; White et al., 1992; Hennemann et al., 1992a–c; Kanter et al., 1992). All of the connexins have four putative membrane-spanning domains with both the amino and the carboxyl termini residing on the cytoplasmic side of the membrane (Zimmer et al., 1987; Goodenough et al., 1988; Milks et al., 1988; Yancey et al., 1988). The extracellular and transmembrane-spanning domains are highly conserved. In contrast, the cytoplasmic domains show much less sequence homology (Beyer et al., 1990).

Each gap-junctional channel spans two plasma membranes and is composed of two hemichannels or connexons arranged in series. The hemichannels, in turn, are oligomers of connexins. Recent studies suggest that gap-junctional precursors are present as hemichannels in the plasma membrane before their assembly into gap-junctional channels (Musil and Goodenough, 1991, 1993; Paul et al., 1991; DeVries and Schwartz, 1992; Ebihara and Steiner, 1993; Gupta et al., 1994). Although these hemichannels are normally closed under physiological conditions, there is evidence that certain pharmacological manipulations may cause them to open (DeVries and Schwartz, 1992; Malchow et al., 1994). Furthermore, rat Cx46 or bovine Cx44, when expressed in Xenopus oocytes, induce voltage-gated currents that have been ascribed to hemichannels (Paul et al., 1991; Ebihara and Steiner, 1993; Gupta et al., 1994).

Because of the unusual nature of gap-junctional channels, it has been difficult to characterize and understand their voltage-dependent behavior, ion permeabilities, and modulation. To gain a better understanding of the voltage-dependent behavior of gap-junctional channels, we have characterized and compared the functional properties of two gap-junctional proteins (rat Cx46 and chicken Cx56) that have the ability to form functional hemichannels in the nonjunctional plasma membrane of solitary oocytes as well as gap-junctional channels in paired oocytes. Our results showed that the voltage-dependent behavior of the Cx56- and Cx46-induced nonjunctional channels could account remarkably well for the distinct behavior of the gap-junctional channels formed by Cx56 and Cx46. These results suggest that many of the voltage-dependent properties of the hemi-gap-junctional channels are retained by the homotypic gap-junctional channels.

MATERIALS AND METHODS

In vitro transcription and translation of connexins

A DNA fragment containing the entire coding region of chicken Cx56 was excised from pBluescript (Stratagene, La Jolla, Ca) by EcoRI digestion and subcloned into the EcoRI site of the RNA expression vector pSP64T II between the 5' and 3' noncoding regions of Xenopus β-globin. This plasmid was derived from pSP64T (Krieg and Melton, 1984) by deleting the EcoRI site in the polycloning region and replacing the BglII site with an EcoRI site. The pSP64T plasmid containing the coding sequence of Cx46 was a gift of Dr. D. A. Goodenough (Harvard University, Boston, MA). The constructs were linearized with an appropriate restriction enzyme and transcribed in vitro with SP6 polymerase as described previously (Swenson et al., 1989). The cRNAs were then aliquoted and stored at −70°C. To verify that the cRNAs could be translated in vitro, samples of the cRNAs were translated

in a rabbit reticulocyte lysate (Life Technologies, Gaithersburg, MD) in the presence of [^{35}S]methionine according to the manufacturer's instructions. The radioactively labeled translation products were separated on a 12% SDS-polyacrylamide gel, fixed in 10% acetic acid, 40% methanol for 30 min at room temperature and detected by fluorography.

Preparation of *Xenopus* oocytes and injection of cRNA

Oocytes were prepared and injected with cRNA as described previously (Ebihara and Steiner, 1993). For the cell-to-cell coupling assay, oocytes were injected with 40 nl of a 0.1 ng/ml solution of an oligonucleotide antisense to mRNA for *Xenopus* Cx38 24 h before injection with cRNA. This treatment has been shown previously to drastically reduce endogenous coupling (Barrio et al., 1991; Hennemann et al., 1992c; Bruzzone et al., 1993).

Immunoblotting

Whole lenses from chickens at embryonic day 18 were homogenized in 0.5 mM EDTA, 2 mM PMSF, in PBS (10 mM sodium phosphate, 150 mM NaCl, pH 7.4). Preparations enriched in plasma membranes from *Xenopus* oocytes were prepared according to White et al. (1992) and Gupta et al. (1994). Immunoblots were performed as described previously (Berthoud et al., 1994).

Electrophysiology

Transmembrane currents were recorded in single oocytes using a two-microelectrode voltage-clamp technique. The current and voltage electrodes had resistances of 0.2–1 MΩ and were filled with 1.5 M KCl, 10 mM EGTA, and 10 mM HEPES (pH 7.4). To prevent KCl from leaking out of the electrodes, the tips of the electrodes were back-filled with a cushion of 1% agar in 1.5 M KCl (Schreibmayer et al., 1993). All experiments were performed at 20–22°C. The bath solution contained modified Barth's solution (MBS): 88 mM NaCl, 1 mM KCl, 2.4 mM NaHCO$_3$, 15 mM HEPES, 0.3 mM Ca(NO$_3$)$_2$, 0.41 mM CaCl$_2$, and 0.82 mM MgSO$_4$, pH 7.4. In the experiments comparing the voltage-dependent properties of the nonjunctional and junctional currents, the oocytes were bathed in "pseudo-intracellular" solution containing (in mM): 89 KCl, 2.4 NaHCO$_3$, 15 HEPES, 0 added CaCl$_2$, 0.8 MgCl$_2$, and 0.2 EGTA, pH 7.4. Control oocytes from each batch

were tested for the presence of endogenous currents, and only those batches with low levels of endogenous currents were used here. Details about the voltage clamp apparatus, data collection and analysis have been described previously (Ebihara and Steiner, 1993). The currents were corrected for a linear leakage component, which was estimated from the I-V relation between −40 and −10 mV. In the reduced calcium experiments, the connexin-induced nonjunctional current was determined as the difference between the current recorded in the absence and presence of cobalt ions. Control experiments showed that the cobalt difference current in noninjected oocytes was very small and therefore could be neglected.

For the cell-to-cell coupling assay, oocytes were devitellinized following the procedure of Methfessel et al. (1986), paired, and incubated in MBS containing either 3 mM Ca^{2+} or 1 mM Co^{2+} at 18°C for 15–24 h before recording. The oocyte pairs were assayed for coupling using a dual two-microelectrode voltage clamp technique (Spray et al., 1981). Only oocyte pairs with junctional conductances less than ~10 μS were selected for data analysis. Families of junctional currents were generated by applying transjunctional voltage clamp steps to ±90 mV in 10-mV increments from a holding potential of −40 mV. Values for initial currents were determined by fitting the current traces to the sum of two exponentials and extrapolating to zero. Values for the steady-state currents were determined at the end of the 8-s pulse. $G_{j\infty}$ was normalized in each cell pair to the value of G_j at $V_j = 0$ mV. $G_j(V_j = 0$ mV) was estimated from the linear region of the initial I_j-V_j curve.

RESULTS

Immunoblotting

The expression of Cx56 in Cx56 cRNA-injected oocytes was verified by immunoblotting of plasma membrane-enriched preparations using affinity-purified anti-Cx56 peptide antibodies (Fig. 1 *A*) (Berthoud et al., 1994). A major immunoreactive band with the same electrophoretic mobility as in vitro translated Cx56 and several other bands were observed in these preparations; most of these bands had faster electrophoretic mobilities than the major band, and might represent degradation products. In contrast, a homogenate from the 18th embryonic day chicken lens contained multiple Cx56 bands with apparent molecular masses between 67–90
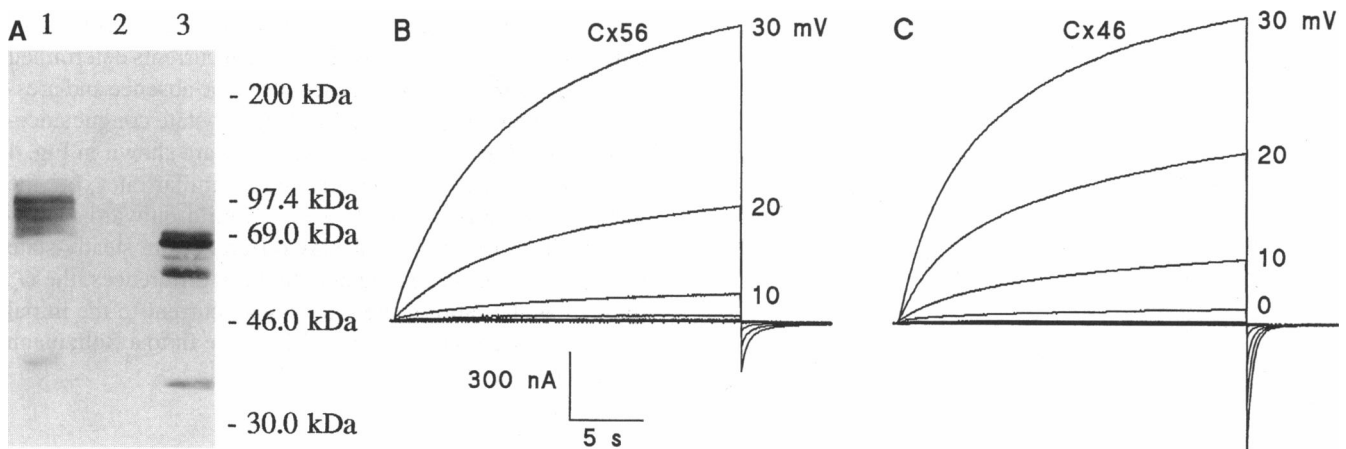

FIGURE 1   (*A*) Immunoblot analysis of Cx56 in *Xenopus* oocytes, and chicken lens. A whole lens homogenate from the 18th embryonic day chicken was run as a control (lane 1). Plasma membrane-enriched preparations from noninjected or Cx56 cRNA-injected *Xenopus* oocytes were run in lanes 2 and 3, respectively. The electrophoretic mobilities of the molecular weight standards are indicated on the left of the figure. (*B, C*) connexin-induced, nonjunctional currents in single oocytes injected with Cx56 (*B*) or Cx46 (*C*) cRNA. Whole cell currents in oocytes were recorded in the two microelectrode voltage clamp configuration. Voltage clamp steps were applied in increments of 10 mV between −40, and +30 mV from a holding potential of −40 mV; the interpulse interval was 80 s.

kDa as described previously (Berthoud et al., 1994). No immunoreactive bands were detected in noninjected oocytes.

Functional properties of a Cx56-induced nonjunctional current

Depolarization of Cx56 cRNA-injected oocytes to potentials greater than −10 mV evoked a slowly activating outward current (Fig. 1 *B*). A similar current was observed in oocytes injected with cRNA for Cx46 (Fig. 1 *C*), but not in control oocytes (not shown). On repolarization to −40 mV, biphasic inward tail currents were observed. Initial current-voltage relationships for the connexin-induced currents were obtained from the tail currents (Fig. 2). Both currents reversed polarity between −5 and −10 mV. The Cx56-induced current was outwardly rectifying at potentials positive to the reversal potential, whereas the current-voltage relationship for the Cx46-induced current was linear over the same range. Similar results were obtained in eight other experiments. To determine the relative permeability of different cations and anions in the Cx56-induced channels, ion substitution experiments were performed. When TEA was substituted for sodium in the external bathing solution, the reversal potential shifted to −26 mV ($n = 5$). Substitution of potassium for sodium or gluconate for chloride had no significant effect on the reversal potential. Interestingly, partial substitution of chloride by gluconate did cause a large increase in the amplitude of the Cx56-induced current, probably due to chelation of external calcium. These findings are similar to those previously obtained for other putative hemi-gap-junctional currents (Ebihara and Steiner, 1993; DeVries and Schwartz, 1992; Malchow et al., 1994; Gupta et al., 1994) and suggest that the Cx56-induced current is either a nonselective cation current or a generally nonselective current that cannot discriminate between chloride and gluconate.
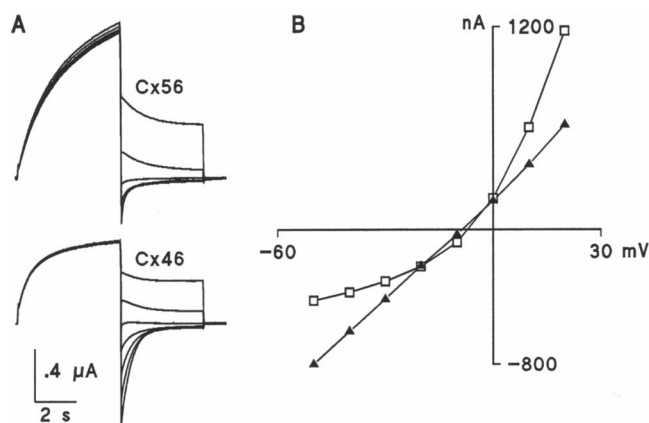
A key feature of putative hemi-gap-junctional channels is that they are blocked by physiological concentrations of extracellular calcium ions (Ebihara and Steiner, 1993; DeVries and Schwartz, 1992). Removal of external calcium caused a dramatic increase in the amplitude of the Cx56-induced current and accelerated the time course of activation (Fig. 3). These effects were reversible on washout. Conductance changes of similar magnitude and properties were not observed in control, noninjected oocytes. Increasing external calcium to 3 mM or adding 1 mM cobalt to the bath completely blocked the Cx56-induced current

Comparison of the voltage-dependent properties of the connexin-induced nonjunctional and junctional channels

It has been observed previously that in the absence of external calcium, the kinetics of deactivation and steady-state voltage dependence of the Cx46-induced nonjunctional current more closely resemble those of the Cx46 gap-junctional conductance (Ebihara and Steiner, 1993). One possible explanation for this finding is that calcium binds to a site within the external mouth of the connexons, thus preventing them from opening. When two connexons join to form an intercellular channel, the binding site(s) for extracellular calcium becomes inaccessible or incapable of affecting channel closure.

To investigate whether the voltage-dependent properties of single connexons could account for the behavior of the intercellular channels, we characterized the voltage-dependent properties of the connexin-induced, nonjunctional currents in oocytes bathed in a "pseudo-intracellular" solution containing high [K⁺] and reduced [Ca⁺²], and compared them with the Cx56 and Cx46 gap-junctional currents. Single oocytes were injected with cRNA for Cx56 or Cx46, bathed in "pseudo-intracellular" solution, and voltage-clamped to a series of values between −60 and 20 mV from a holding potential of −6 mV. The same pulse protocol was then repeated in the presence of 1 mM cobalt to block the connexin-induced currents. The connexin-induced currents determined from the difference between currents in the absence and presence of cobalt and the normalized steady-state conductance-voltage relationship for Cx56 and Cx46 are shown in Fig. 4 *A–D*. The currents both deactivated at similar rates, but the initial I-V relation for Cx56 showed mild outward rectification. The currents also display differences in steady-state voltage dependence. To quantitate these differences, the G_∞ (plotted as the ratio of the steady-state current to the initial current) versus voltage relationships were fit to a Boltzmann equation of the form:

$$G_\infty(V) = G_{min}$$
$$+ (G_{max} - G_{min})/(1 + \exp(-A *(V - V_o))). \quad (1)$$

The G_∞-V curve for Cx56 ($n = 4$) had a midpoint (V_o) of −19.3 mV and a slope factor (A) of 0.095. At a membrane potential of 0 mV, the current was approximately 80% activated. The G_∞-V curve for Cx46 ($n = 4$) had a midpoint (V_o)

FIGURE 2 (*A*) Initial current versus voltage relationships for Cx56 and Cx46. Oocytes injected with Cx56 or Cx46 cRNA were depolarized to +20 mV for 24 s from a holding potential of −10 mV and then repolarized to potentials between −50 and 20 mV in increments of 10 mV. (*B*) The initial amplitude of the tail current was measured 30 ms after the beginning of the test pulse and plotted as a function of transmembrane potential. Cx56 (□); Cx46 (▲).

FIGURE 3   Effect of changing external calcium on the Cx56-induced currents. (A) Transmembrane currents were recorded in Cx56 cRNA-injected oocytes that were sequentially superfused with solutions containing different calcium ion concentrations. Voltage-clamp steps were applied in 10 mV increments between −60 and +30 mV from a holding potential of −60 mV. The composition of the 0 mM calcium solution was the same as that of the modified Barth's solution with 0.2 mM EGTA, 0.8 mM MgSO$_4$, and no added calcium, and that of the 0.7 mM calcium contained 0.7 mM CaCl$_2$ and 0.8 mM MgSO$_4$. (B) The current at the end of each pulse in A was plotted as a function of transmembrane potential for nominal extracellular concentrations of calcium ions of 0 mM (■) and 0.7 mM (▲).
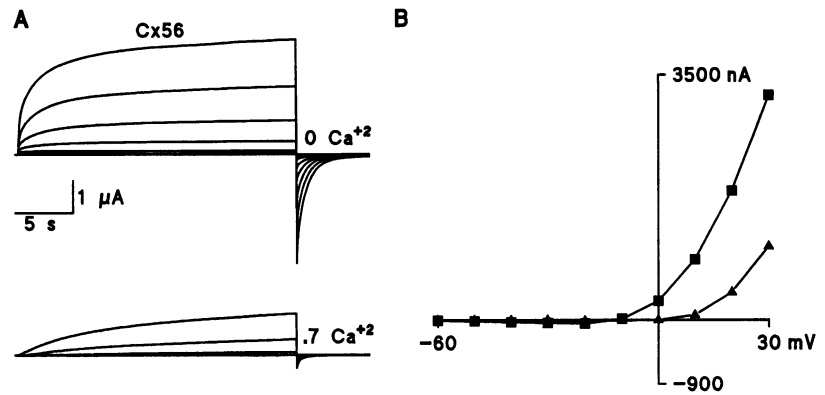
of −30.4 mV, an A of 0.119, and was fully activated at 0 mV. The parameters for Cx46 were similar to those reported previously (Ebihara and Steiner, 1993).

To characterize the voltage-dependent properties of Cx56 and Cx46 gap-junctional channels, connexin-injected *Xenopus* oocytes were paired (Dahl et al., 1987) and assayed for coupling using a dual two-microelectrode voltage clamp technique. Background endogenous coupling was prevented by pre-injecting the oocytes with antisense oligonucleotides for *Xenopus* Cx38 24 h before pairing (Barrio et al., 1991; Bruzzone et al., 1993). An example of junctional currents developed in Cx56 cRNA-injected oocyte pairs is shown in Fig. 4 C (*top*). The junctional currents decayed slowly to a new steady-state level on application of depolarizing or hyperpolarizing transjunctional voltage clamp steps (V_j) to potentials greater than ±30 mV. The relationship between normalized steady-state junctional conductance ($G_{j\infty}$) and V_j is shown in Fig. 4 C (*bottom*). $G_{j\infty}$ declined symmetrically at positive and negative V_j values. The mean $G_{j\infty}$-V_j relation ($n = 3$) could be described by a Boltzmann function with $A = \pm0.07$, $V_o = \pm49.5$ mV, $G_{jmax} = 1.0$, and $G_{jmin} = 0.125$. Junctional currents between oocytes expressing Cx46 also decreased in a time- and voltage-dependent manner (Fig. 4 D). The rates of decay of the Cx46 and Cx56 junctional currents were similar. However, the $G_{j\infty}$-V_j relation for the Cx46 gap-junctional channels was less sensitive to voltage than for the Cx56 channels. Similar findings for Cx46 gap-junctional channels have been reported recently by White et al. (1994a).

To predict the voltage-dependent properties of the gap-junctional channels from the nonjunctional current data, the system was modeled with the coupled reaction scheme outlined below (Harris et al., 1981):

$$C_1 \leftrightarrow O \leftrightarrow C_2$$
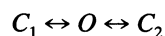
In this simplified representation, there are two gates in series that close the channel from a single open state (O) to two independent groups of one or more closed states signified by (C_1) and (C_2). Because the voltage gating for potentials of either polarity is symmetrical about 0 mV, the gates must close for potentials of opposite polarities and have identical rate constants. Furthermore, it is assumed that the rate con-

stants are intrinsic to each hemichannel and that half of the transjunctional voltage drop occurs across each gate.

In the case of Cx46, the nonjunctional current data indicate that the hemichannels are fully activated at 0 mV. Therefore, when a transjunctional voltage is applied to the cell pair, the time course of inactivation of the gap-junctional conductance should be determined solely by the intrinsic properties of the hemichannel that closes. To test this prediction, the inactivation kinetics of the Cx46 gap-junctional channels were compared with the deactivation kinetics of the nonjunctional current. In Fig. 5 A, Cx46-induced nonjunctional currents recorded in response to hyperpolarizing steps to −10, −20, −30, −40, and −50 mV were superimposed on a series of junctional current traces recorded from a Cx46/Cx46 pair in response to transjunctional voltage clamp steps to 0, −20, −40, −60, −80, and −100 mV, respectively. The time courses of the two sets of current traces are in excellent agreement.

In the case of Cx56, the hemichannels are not fully activated at 0 mV. The model predicts that junctional channels originally in state C_1 must open before they can close to state C_2 and vice versa. Because at 0 mV, ~10% of the Cx56 gap-junctional channels are predicted to be in state C_1, the time course of activation is not expected to be predicted perfectly by the time course of deactivation of the hemichannel current. However, the effect of this delayed component on the overall time course of inactivation of the junctional current should be minimal, as shown experimentally in Fig. 5 B.

Another prediction of the model is that the steady-state G_j-V_j relationship can be determined from the product of the probabilities that the two hemichannels are open for a given transjunctional voltage difference. This hypothesis was tested by comparing the predicted $G_{j\infty}$-V_j relationships for Cx56 and for Cx46 with the experimental data (Fig. 5, C and D). The model predicts that the $G_{j\infty}$-V_j relationships for Cx56 and Cx46 will have similar shapes but that the relationship for Cx56 will be significantly more sensitive to transjunctional voltage. These predictions are in good agreement with the experimental data. An alternative model in which the voltage difference across each gate is assumed to be state-dependent cannot be excluded on the basis of our experimental data.
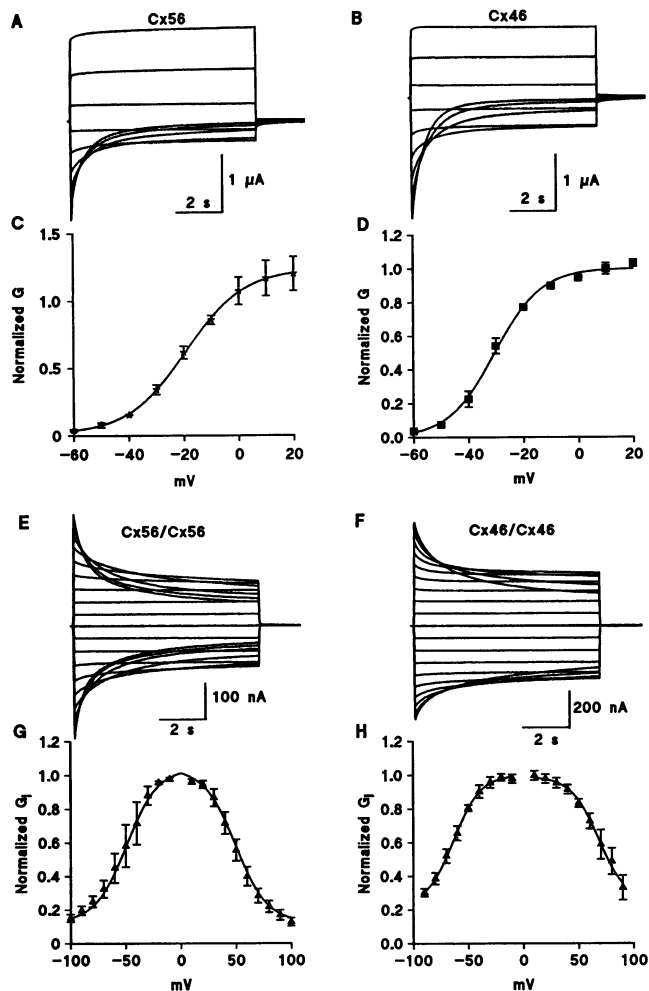
FIGURE 4 Nonjunctional and junctional channels composed of Cx56 and Cx46 exhibit distinct voltage-dependent properties. (*A*, *B*) connexin-induced nonjunctional currents recorded from Cx56 (*A*) and Cx46 (*B*) cRNA-injected oocytes in "pseudo-intracellular" solution. The membrane potential was stepped from the equilibrium potential of the nonjunctional current ($\sim$-6 mV) to a series of voltages between –60 and +20 mV in increments of 10 mV. Then 1 mM $CoCl_2$ was added to the external solution and the pulse protocol was repeated. The connexin-induced current shown corresponds to the difference between the current recorded in the absence and presence of cobalt ions. (*C*, *D*) Plots of the normalized $G_\infty-V$ relation for Cx56 (*C*) and Cx46 (*D*). The solid lines are the best fit of the experimental data to a Boltzmann equation with $A = 0.095$, $V_o = -19.3$ mV, $G_{max} = 1.23$, $G_{min} = 0.0124$ for Cx56 ($n = 4$), and $A = 0.119$, $V_o = -30.4$ mV, $G_{max} = 1.0$, $G_{min} = 0$ for Cx46 ($n = 4$). (*E*, *F*) Gap junctional current traces recorded from homotypic Cx56 (*E*) and Cx46 (*F*) oocyte pairs. Families of gap-junctional currents were generated by applying transjunctional voltage clamp steps to ±90 mV in 10-mV increments from a holding potential of –40 mV. (*G*, *H*) Plots of the $G_{j\infty}-V_j$ relationship for Cx56 (*G*) and Cx46 (*H*) cell pairs. The solid lines are the best fit of the experimental data to a Boltzmann equation. In the case of the Cx56/Cx56 pairs, the Boltzmann parameters are: $A = \pm0.07$, $V_o = \pm49.5$ mV, $G_{max} = 1.04$, and $G_{jmin} = 0.125$ for positive and negative Vs. Results are shown as means $\pm$ SEM of three pairs, whose conductance is 7.7 $\pm$ 4.1 μS. In the case of Cx46/Cx46 pairs, the Boltzmann parameters are: $A = -0.08$, $V_o = 68$ mV, $G_{max} = 0.99$, $G_{min} = 0.24$ for positive V_js, and $A = 0.08$, $V_o = -64$ mV, $G_{max} = 1.0$, $G_{min} = 0.22$ for negative V_js. Results are shown as means $\pm$ SEM of four pairs, whose conductance is 5.58 $\pm$ 4.6 μS.
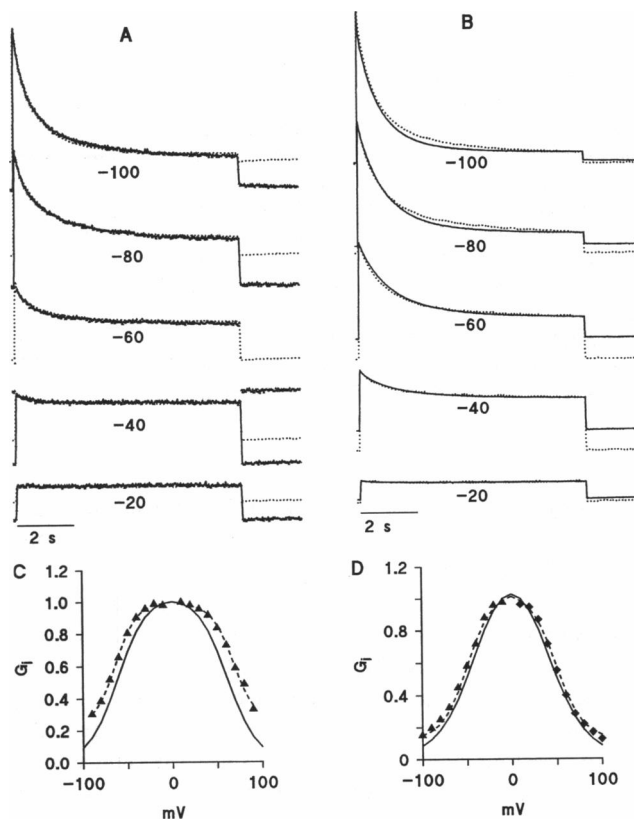
FIGURE 5 (*A*, *B*) Comparison of the kinetics of inactivation of the junctional currents with the kinetics of deactivation of the nonjunctional currents recorded in "pseudo-intracellular" solution. Cx46 (*A*)- and Cx56 (*B*)-induced, nonjunctional current traces at –10, –20, –30, –40, and –50 mV were scaled so that the amplitude of the tail current was the same size as the amplitude of the inactivating component of the junctional current and superimposed on a series of junctional current traces recorded from a Cx46/Cx46 or Cx56/Cx56 pair in response to transjunctional voltages to –20, –40, –60, –80, and –100 mV, respectively. The dotted lines are the scaled nonjunctional current traces. (*C*, *D*) The steady-state G_j-V_j curves predicted by the model (——) for Cx46 (*C*) and Cx56 (*D*) are compared with the best fit of the experimental data to a Boltzmann function (- - - -). The predicted steady-state G_j-V_j curves were computed from the nonjunctional current data as:

$$G_{j\infty} = \frac{P_{\infty,1}(V_j/2)P_{\infty,2}(V_j/2)}{P_{\infty,1}(0)P_{\infty,2}(0)},$$

where $G_{j\infty}$ is the normalized steady-state junctional conductance, $P_{\infty,n}$ is the steady-state probability that hemichannel 1 or 2 is open, and V_j is the transmembrane voltage. P_∞ was estimated from the connexin-induced nonjunctional conductance data by fitting the normalized conductance-voltage curves to a Boltzmann relation as shown in Fig. 4, *G* and *H*. In the case of homotypic channels, the $P_\infty-V$ curves for hemichannel 1 and 2 were assumed be symmetrical about $V = 0$.

A third prediction is that the time course of recovery of the gap-junctional conductance after a large transjunctional voltage clamp step will be determined by the time course of activation of the nonjunctional current. To test this prediction, the time course of recovery of the Cx46 gap-junctional current was measured using a double-pulse protocol as shown in Fig. 6 *A*. The normalized junctional current measured during the second pulse was then plotted as a function

Ebihara et al.
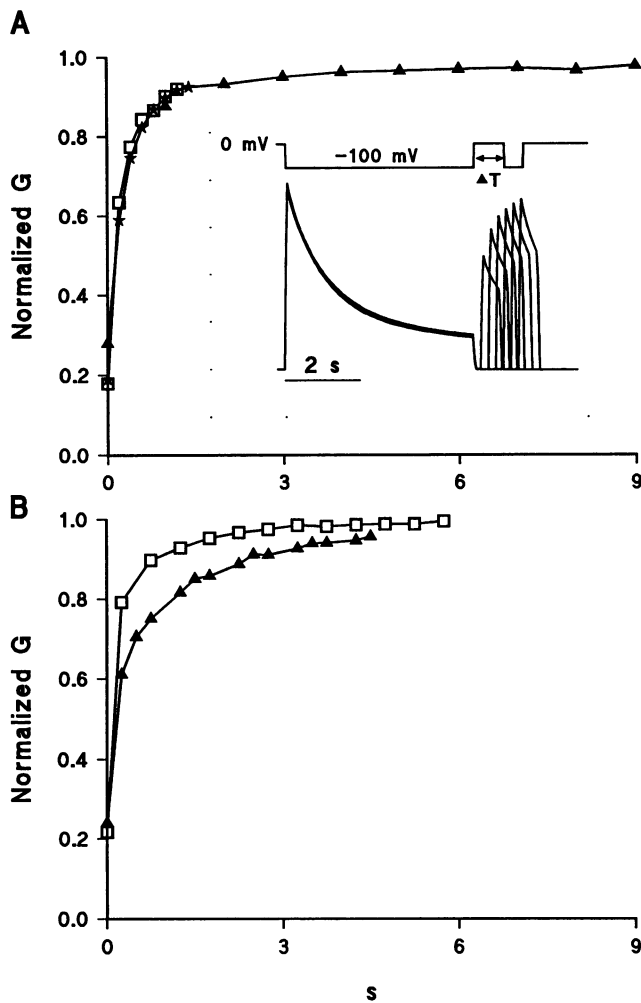Behavior of Connexin56 and Connexin46 Channels
1801

FIGURE 6 The time course of recovery of the gap-junctional conductance can be predicted from the time course of activation of the connexin-induced nonjunctional current. (A) Comparison of the time course of recovery of the Cx46 gap-junctional conductance and the time course of activation of the Cx46-induced nonjunctional current. The time course of recovery of the Cx46 gap-junctional current was measured using a double-pulse protocol as shown in the inset. The peak junctional current measured during the second pulse (normalized with respect to the peak junctional current recorded during the first pulse) was plotted as a function of interpulse duration (□). The time course of activation of the Cx46-induced nonjunctional current in "pseudo-intracellular solution" was determined by a similar pulse protocol in which two hyperpolarizing voltage clamp steps to −40 mV were applied in succession from a holding potential of −4 mV. The current at the end of the second pulse (normalized with respect to the current recorded at the end of the conditioning pulse) was plotted as a function of interpulse interval (▲). (B) Comparison of the time course of recovery of the Cx56 gap-junctional conductance (□) and the time course of activation of the Cx56-induced nonjunctional current (▲).

of interpulse duration (*open squares*) and compared with the time course of activation of the Cx46-induced nonjunctional current (*solid symbols*). The two curves are nearly superimposable. Hence, the model can account for the time course of recovery of the junctional conductance. In the case of Cx56, the time course of the two processes were similar but not identical (Fig. 6 *B*). The Cx56 gap-junctional current (*open squares*) rose to a new steady-

state level more rapidly than the Cx56 nonjunctional current (*solid triangles*).

DISCUSSION

This study shows that Cx56 forms ion channels in the nonjunctional membrane of oocytes as well as gap-junctional channels between oocyte pairs. The voltage-dependent properties of the nonjunctional and junctional channels formed by Cx56 are distinct from those formed by Cx46. Furthermore, the behavior of the nonjunctional channels formed by Cx56 and Cx46 in external solutions containing reduced calcium ions could account remarkably well for the behavior of the intercellular channels formed by Cx56 and Cx46. Taken together, these results strongly suggest that the nonjunctional channels induced by Cx56 and Cx46 are single connexons or hemichannels rather than some other oligomeric form.

The *Xenopus* oocyte expression system has been used to study the functional properties of a number of different connexins including Cx32, Cx26, Cx43, Cx40, Cx38, Cx37, Cx50, Cx46, Cx56, and Cx44 (Dahl et al., 1987; Barrio et al., 1991; Verselis et al., 1994; Swenson et al., 1989; Bruzzone et al., 1993; Ebihara et al., 1989; Henneman et al., 1992c; White et al., 1994a, b; Gupta et al., 1994). Of these connexins, only rat Cx46, bovine Cx44, and chicken Cx56 have been reported to form functional hemichannels in the nonjunctional plasma membrane of oocytes. Comparison of the predicted amino acid sequence of Cx56, Cx46, and Cx44 shows that these three connexins are more closely related to each other than to other members of the connexin family. Cx56 contains 62 and 63% identical amino acids to Cx46 and Cx44, respectively. This homology is most striking in the region of the proteins corresponding to the putative first and second transmembrane-spanning domains and first extracellular domain. Thus, these regions of the protein may be responsible for the unique ability of these connexins to form functional hemichannels in oocytes.

It has been shown previously that rat Cx46, bovine Cx44, and chicken Cx56 are phosphoproteins that are detected in immunoblots of lens homogenates as multiple bands (Paul et al., 1991; Gupta et al., 1994; Berthoud et al., 1994). When synthesized in *Xenopus* oocytes, these proteins have the same electrophoretic mobilities as the in vitro translated proteins (Paul et al., 1991; Gupta et al., 1994) (this study). These observations suggest that the connexins are not modified identically in the two cell types.

The high input impedance of the lens fiber cells indicates that if the connexins exist as hemichannels in the nonjunctional plasma membrane, they must be closed. The difference in behavior of Cx46, Cx44, and Cx56 in oocytes and the lens could be due to differences in posttranslational processing. Alternatively, the native channels may contain addition subunits that are missing from the oocyte expression system. It would be interesting to determine whether these connexins can form functional hemichannels in stably transfected mammalian cell lines.

Mechanism underlying the voltage-dependent behavior of gap-junctional channels

Our data suggest that the voltage-dependent properties of homotypic Cx46 and Cx56 gap-junctional channels can be predicted from the behavior of their hemi-gap-junctional channels. These conclusions are consistent with a study by DeVries and Schwartz (1992) on a putative hemi-gap-junctional current in catfish horizontal cells which indicated that the voltage-dependent behavior of the gap-junctional channels between teleost horizontal cells could be predicted from the voltage-dependent properties of the hemi-gap-junctional current. It is also interesting to note that the voltage-dependent behavior of the hemichannels shows a striking resemblance to the behavior of a Cx26 mutant connexon incorporated into heterotypic gap-junctional channels with either Cx26 or Cx32 (Suchyna et al., 1993).

Although the behavior of the hemichannels can account remarkably well for the properties of the gap-junctional channels in our system, there is evidence that suggests that the situation is more complicated under other conditions. Barrio et al. (1991) showed that heterotypic gap-junctional channels formed from Cx32 and Cx26 in paired oocytes exhibit novel voltage-dependent behavior that has been interpreted as arising from opposite voltage-gating polarities of the two connexons, with the Cx26 connexon closing when its cytoplasmic end is relatively positive and the Cx32 connexon closing for relative negativity (Verselis et al., 1994). Recently, White et al. (1994b) showed that heterotypic gap-junctional channels formed from Cx46 and Cx32 in paired oocytes exhibit voltage sensitivities that are similar to those observed for the heterotypic Cx26/Cx32 channels, suggesting that the Cx46 connexons in heterotypic Cx32/Cx46 channels must also close for relative positivity. These investigators proposed that the novel behavior of the heterotypic gap-junctional channels is due to allosteric interactions between opposing connexons that results in a reversal of polarity of voltage gating of the Cx46 connexons. The difference between this study and our results suggests that the voltage-dependent behavior of the Cx46 connexons is modified by interaction with the opposing connexon in heterotypic Cx46/Cx32 channels but not in homotypic Cx46/Cx46 channels.

In summary, we have shown that Cx56 and Cx46 form functional hemichannels in the nonjunctional plasma membrane of oocytes. Many of the properties of the hemichannels are retained by the gap-junctional channels. These results suggest that by studying the properties of hemi-gap-junctional channels in single oocytes, it may be possible to obtain a clearer understanding of the mechanisms underlying the voltage-dependent behavior and modulation of gap-junctional channels.

REFERENCES

Barrio, L. C., T. Suchyna, T. Bargiello, L. X. Xu, R. Roginsky, M. V. L. Bennett, and B. J. Nicholson. 1991. Voltage dependence of homo- and hetero-typic cx26 and cx32 gap junctions expressed in Xenopus oocytes. Proc. Natl. Acad. Sci. USA. 88:8410–8414.

Berthoud, V. M., A. J. Cook, and E. C. Beyer. 1994. Characterization of the gap junction protein connexin56 in the chicken lens by immunofluorescence and immunoblotting. Invest. Ophthalmol. Vis. Sci. In press.

Beyer, E. C., D. L. Paul, and D. A. Goodenough. 1987. Connexin43: a protein from rat heart homologous to a gap junction protein from liver. J. Cell Biol. 105:2621–2629.

Beyer, E. C., D. L. Paul, and D. A. Goodenough. 1990. Connexin family of gap junction proteins. J. Membr. Biol. 116:187–194.

Bruzzone, R., J.-A. Haeffliger, R. L. Gimlich, and D. L. Paul. 1993. Connexin40, a component of gap junctions in vascular endothelium, is restricted in its ability to interact with other connexins. Mol. Biol. Cell. 4:7–20.

Dahl, G., T. Miller, D. L. Paul, R. Voellmy, and R. Werner. 1987. Expression of functional cell-cell channels from cloned rat liver gap junction complementary cDNA. Science. 236:1290–1293.

DeVries, S. H., and E. A. Schwartz. 1991. Hemi-gap junction channels in solitary horizontal cells of the catfish retina. J. Physiol. 455:201–230.

Ebihara, L., and E. Steiner. 1993. Properties of a nonjunctional current expressed from a rat connexin46 cDNA in Xenopus oocytes. J. Gen. Physiol. 102:59–74.

Goodenough, D. A., D. L. Paul, and L. Jesaitis. 1988. Topological distribution of two connexin32 antigenic sites in intact and split rodent hepatocyte gap junctions. J. Cell Biol. 107:1817–1824.

Gupta, V. K., V. M. Berthoud, N. Atal, J. A. Jarillo, L. C. Barrio, E. C. Beyer. 1994. Bovine Connexin44, a lens gap junction protein: molecular cloning, immunological characterization, and functional expression. Invest. Ophthalmol. Vis. Sci. In press.

Hennemann, H., E. Dahl, J. B. White, H.-J. Schwarz, P. A. Lalley, S. Chang, B. J. Nicholson, and K. Willecke. 1992a. Two gap junction genes, connexin 31.1 and 30.3 are closely linked on mouse chromosome 4 preferentially expressed in skin. J. Biol. Chem. 267:17225–17233.

Hennemann, H., H.-J. Schwarz, and K. Willecke. 1992b. Characterization of gap junction genes expressed in F9 embryonic carcinoma cells: molecular cloning of mouse connexin31 and -45 cDNAs. Eur. J. Cell Biol. 57:51–58.

Hennemann, H., T. Suchyna, H. Lichtenberg-Frate, S. Jungbluth, E. Dahl, H.-J. Schwarz, B. J. Nicholson, and K. Willecke. 1992. c. Molecular cloning and functional expression of mouse connexin40, a second gap junction gene preferentially expressed in lung. J. Cell Biol. 117: 1299–1310.

Kanter, H. L., J. E. Saffitz, and E. C. Beyer. 1992. Cardiac myocytes express multiple gap junction proteins. Circ. Res. 70:438–444.

Krieg, P. A., and D. A. Melton. 1984. Functional messenger RNAs are produced by SP6 in vitro transcription of cloned cDNAs. Nucleic Acids Res. 12:7057–7070.

Malchow, R. P., H. Qian, and H. Ripps. 1994. A novel action of quinine and quinidine on the membrane conductance of neurons from the vertebrate retina. J. Gen. Physiol. 104:1039–1055.

Methfessel, C., V. Witzemann, T. Takahashi, M. Mishina, S. Numa, and B. Sakmann. 1986. Patch clamp measurements on Xenopus laevis oocytes: currents through endogenous channels and implanted acetylcholine receptor and sodium channels. Pflügers Arch. 407:577–588.

Milks, L. C., N. M. Kumar, R. Houghten, N. Unwin, and N, B. Gilula. 1988. Topology of the 32-kd liver gap junction protein determined by site-directed antibody localizations. EMBO J. 7:2967–2975.

Musil, L. S., and D. A. Goodenough. 1991. Biochemical analysis of connexin43 intracellular transport, phosphorylation, and assembly into gap junctional plaques. J. Cell Biol. 115:1357–1374.

Musil, L. S., and D. A. Goodenough. 1993. Multisubunit assembly of an integral plasma membrane channel protein, gap junction connexin43, occurs after exit from ER. Cell. 74:1065–1077.

Paul, D. L. 1986. Molecular cloning of cDNA for rat liver gap junction protein. J. Cell Biol. 103:123–134.

Paul, D. L., L. Ebihara, L. J. Takemoto, K. I. Swenson, and D. A. Goodenough. 1991. Connexin46, a novel lens gap junction protein, induces

voltage-gated currents in nonjunctional plasma membrane of *Xenopus* oocytes. *J. Cell Biol.* 115:1077–1089.

Rup, D. M., R. D. Veenstra, H.-Z. Wang, P. R. Brink, and E. C. Beyer. 1993. Chick connexin-56, a novel lens gap junction protein. *J. Biol. Chem.* 268:706–712.

Schreibmayer, W., N. Dascal, N. Davidson, and H. Lester. 1993. Improvements in the two-electrode voltage clamp technique of *Xenopus laevis* oocytes for modulation studies. *Biophys. J.* 64:393a. (Abstr.)

Spray, D. C., A. L. Harris, and M. V. L. Bennett. 1981. Equilibrium properties of voltage dependent junctional conductance. *J. Gen. Physiol.* 77: 77–93.

Suchyna, T., L. X. Xu, F. Gao, C. R. Fourtner, and B. J. Nicholson. 1993. Identification of a proline residue as a transduction element involved in the voltage gating of gap junctions. *Nature.* 365:847–849.

Swenson, K. I., J. R. Jordan, E. C. Beyer, and D. L. Paul. 1989. Formation of gap junctions by expression of connexins in *Xenopus* oocyte pairs. *Cell.* 57:145–155.

Verselis, V. K., C. S. Ginter, and T. A. Bargiello. 1994. Opposite voltage gating polarities of two closely related connexins. *Nature.* 368:348–351.

White, T. W., R. Bruzzone, D. A. Goodenough, and D. L. Paul. 1992. Mouse Cx50, a functional member of the connexin family of gap junction proteins is the lens fiber protein, MP70. *Mol. Biol. Cell.* 3:711–720.

White, T. W., R. Bruzzone, S. Wolfram, D. L. Paul, and D. A. Goodenough. 1994a. Selective interactions among the multiple connexin proteins expressed in the vertebrate lens: the second extracellular domain is a determinant of compatibility between connexins. *J. Cell Biol.* 125:879–892.

White, T. W., R. Bruzzone, D. A. Goodenough, and D. L. Paul. 1994b. Voltage gating of connexins. *Nature.* 371:208–209.

Willecke, K., R. Heynkes, E. Dahl, R. Stutenkemper, H. Hennemann, S. Jungbluth, T. Suchyna, and B. J. Nicholson. 1991. Mouse connexin37: cloning and functional expression of a gap junction gene highly expressed in lung. *J. Cell Biol.* 114:1049–1057.

Yancy, S. B., S. A. John, L. Ratneshwar, B. J. Austin, and J.-P. Revel. 1989. The 43-kD polypeptide of heart gap junctions: immunolocalization, topology, and functional domains. *J. Cell Biol.* 108:2241–2254.

Zhang, J.-T., and B. J. Nicholson. 1989. Sequence and tissue distribution of a second protein of hepatic gap junctions, Cx26, as deduced from its cDNA. *J. Cell Biol.* 109:3391–3401.

Zimmer, D. B., C. R. Green, W. H. Evans, and N. B. Gilula. 2624. Topological analysis of the major protein in isolated intact rat liver gap junctions, and gap junction-derived single membrane structures. *J. Biol. Chem.* 262:7751–7763.